Evolution of correlation strength in K_{x}Fe_{2–y}Se_{2} superconductor doped with S

Kefeng Wang (□□□), Hechang Lei (□□□), and C. Petrovic

Phys. Rev. B **84**, 054526 — Published 11 August 2011

DOI: 10.1103/PhysRevB.84.054526

Evolution of correlation strength in $K_xFe_{2-y}Se_2$ superconductor doped with S

Kefeng Wang(王克锋), Hechang Lei(雷和畅), and C. Petrovic
Condensed Matter Physics and Materials Science Department, Brookhaven National Laboratory, Upton, New York 11973 USA
(Dated: June 20, 2011)

We report the evolution of thermal transport properties of $K_xFe_{2-y}Se_2$ with sulfur substitution at Se sites. Sulfur doping suppresses the superconducting T_c. The Seebeck coefficient of all crystals in the low temperature range can be described very well by diffusive thermoelectric response model. The zero-temperature extrapolated value of Seebeck coefficient divided by temperature S/T gradually decreases from $-0.48\mu V/K^2$ to a very small value ~ 0.03 μV/K^2 where T_c is completely suppressed. The normal state electron Sommerfeld term (γ_n) of specific heat also decreases with the increase in sulfur content. The decrease of S/T and γ_n reflects a suppression of the density of states at the Fermi energy, or a change in the Fermi surface that would induce the suppression of correlation strength. Our results imply little relevance of strong electron correlations to superconductivity.

PACS numbers: 74.25.fc, 74.25.fg, 74.20.Mn, 74.70.Xa

I. INTRODUCTION

Superconductivity in pure and F-doped LaFeAsO with T_c up to 26 K has opened a new frontier in the investigation of the novel superconducting materials and mechanisms.[1–3] After an intensive study, superconductivity was discovered in several different types of iron-based materials, including REOFePn (RE=rare earth; Pn=P or As, 1111-type),[4–8] doped AFe_2As_2 (122-type, A=Ba, Sr, Ca),[9–11] Fe_2As-type AFeAs (111-type, A=Li or Na),[12,13] as well as anti-PbO-type Fe(Se,Te) (11-type).[14,15] All have similar structure with the common FeAs-layer units. Most undoped compounds are stripe-like antiferromagnetic (spin density wave, SDW) metals, and the magnetic ordering comes in the vicinity of the structural phase transition from tetragonal to orhtorhombic unit cell. Experimental and theoretical studies suggest that the high-T_c superconductivity in iron-based superconductors is influenced by proximity to SDW phase transition. The doping brings along charge carries that suppress the SDW ordering. It was suggested that the superconductivity may be established via inter-pocket scattering of electrons between the hole pockets and electron pockets, leading to the $s^{\pm}$ pairing.[16–18]

The electron correlation strength in parent materials is therefore one of the central problems in iron-based superconductors. The absence of strong correlations was noted within a tight-binding model and density functional calculations.[19] Moderate electron correlations in arsenic systems were also supported by a small observed ratio between the band-theoretical and experimental kinetic energy.[20,21] Theoretical studies gave an onsite Coulomb repulsion $U < 2$ eV v.s. a Fe conduction bandwidth $W \sim 4$ eV, i.e. $\frac{U}{W} < 0.5$, in 1111 and 122 systems.[22,23] The other line of study indicated that some iron-based superconductors have electron correlations comparable in strength to the cuprates.[24–27] The bad-metal conductivity in the parent compounds was explained by the proximity to a Mott/correlation-induced insulating state and strong electron correlations.[24]

Superconductivity with relatively high $T_c \sim 30$ K was recently reported in a new series of iron-based superconductors $A_xFe_2Se_2$ (A=K,Rb,Cs,Tl).[28–31] These compounds are purely electron-doped and only electron pockets were observed in angle-resolved photoemission experiment.[32–34] Just like other iron-based superconductors,[35] superconductivity in $A_xFe_2Se_2$ is sensitive to the Pn doping and anion height between Fe and Pn layers. Sulfur doping at Se sites suppresses the superconductivity and induces a spin-glass narrow-bandgap semiconductor ground state for complete S substitution.[36,37] The strength of electron correlations in $K_xFe_{2-y}Se_2$ is also highly debated. Some studies indicated the superconductivity is in proximity to a Mott antiferromagnetic insulator, implying strong electron correlations.[38,39] Others argued that the parent compounds are simple band insulators since density functional theory calculation could reproduce the experimental antiferromagnetic ground state with the iron vacancy order.[40] The local density approximation incorporating local interaction (LDA+U) calculation found that the band gap is nearly independent of the value of the Coulomb repulsion U, indicating irrelevance of the Mott physics to the gap formation in neighboring nonmetallic states.[41]

Measurement of thermoelectric properties is an efficient method to characterize the correlation strength in superconductors, as well as the nature and sign of carriers .[25,42,43] In this work we clarify the correlation strength in S doped $K_xFe_{2-y}Se_2$. $K_xFe_{2-y}S_2$ exhibits large Seebeck coefficient at high temperature range which is attributed to the thermally activated carriers over the narrow bandgap. In $K_xFe_{2-y}Se_{2-z}S_z$ ($0 \leq z \leq 2$) single crystal alloys, Seebeck coefficient and the electron Sommerfeld term in specific heat are suppressed, as S enters the $K_xFe_{2-y}Se_2$ superconducting lattice. However, superconductivity survives with relatively high T_c even if electron correlations are considerably reduced, implying little relevance of the strong electron correlation to T_c.

II. EXPERIMENTAL

Single crystals of $K_xFe_{2-y}Se_{2-z}S_z$ were grown from nominal composition K:Fe:Se:S=0.8:2:2-z:z with different S content, as described elsewhere.[36,37] The elemental analysis was performed using an energy-dispersive x-ray spectroscopy (EDX) in a JEOL JSM-6500 scanning electron microscope and in what follows we present the measured stoichiometry values (Table I). Electrical and thermal transport measurements were conducted in Quantum Design PPMS-9. The crystal was cleaved to a rectangular shape with dimension 5×2 mm^2 in the ab-plane and 0.3 mm thickness along the c-axis. Thermoelectric power and thermal conductivity were measured using one-heater-two-thermometer setup which allowed us to determine all transport properties of the crystal with steady-state method. The heat and electrical current were transported within the ab-plane of the crystal oriented by Laue camera, with magnetic field along the c-axis and perpendicular to the heat/electrical current. Silver paint contacts were made directly on the crystal surface providing both good thermal contact and low electrical contact resistance. Since air exposure exceeding 1 hour will result in the surface oxidization, the exposure to air of crystals was less than 20 minutes. The relative error in our measurement for both κ and S was below 5% based on Ni standard measured under identical conditions.

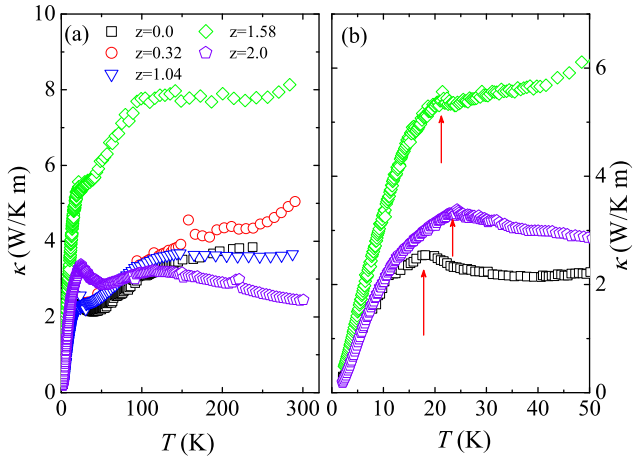

FIG. 1. (Color online) (a) Temperature dependence of thermal conductivity for $K_xFe_{2-y}Se_{2-z}S_z$ in zero magnetic field from 2 K to 300 K. (b) Low temperature thermal conductivity with phonon-related peak indicated by red arrows.

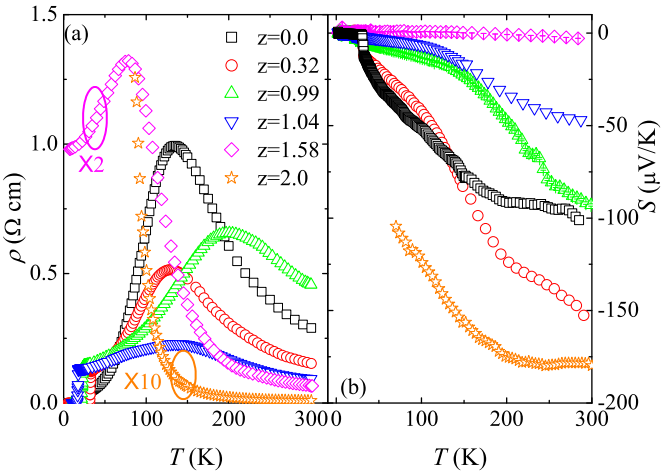

FIG. 2. (Color online) Temperature dependence of resistivity (a) and Seebeck coefficient (b) for $K_xFe_{2-y}Se_{2-z}S_z$ ($z = 0.0, 0.32, 0.99, 1.04$ and 1.58) under zero magnetic field.

III. RESULTS AND DISCUSSIONS

Fig. 1(a) presents temperature dependence of thermal conductivity for $K_xFe_{2-y}Se_{2-z}S_z$ in zero magnetic field from 2 K to 300 K. Thermal conductivity for all crystals exhibits a peak between 15 K and 30 K (Fig. 1(b)). The peak position moves to higher temperature with the increase of sulfur doping (red arrows in Fig. 1(b)). It changes from $\sim$ 17 K in undoped crystal to $\sim$ 25 K in $K_xFe_{2-y}S_2$, and is considered to entirely originate from phonon contribution.[44] This shift is due to the lattice contraction corresponding to the smaller radius of sulfur ion.

With the increase of S concentration, superconducting T_c is suppressed and ultimately vanishes at $z = 1.58$ (Fig. 2(a)). The suppression of T_c is confirmed in Seebeck coefficient $S = 0$ temperature (Fig. 2(b)) since Cooper pairs carry no entropy in the superconducting state. With increase in sulfur doping, the magnitude of Seebeck coefficient decreases significantly for superconducting samples. The Seebeck coefficient for crystal with $z = 1.58$ (which does not exhibit superconducting transition above 1.9 K) is nearly zero in the whole temperature range (the value is ~ -0.75 μV/K at 200 K and ~ 0.06 μV/K at 2 K). For the narrow bandgap semiconductor $K_{0.88}Fe_{1.63}S_2$, ρ and S are beyond the detection limit of our instrument, as shown in Fig. 2(b). The observable Seebeck coefficient appears at $\sim$100 K

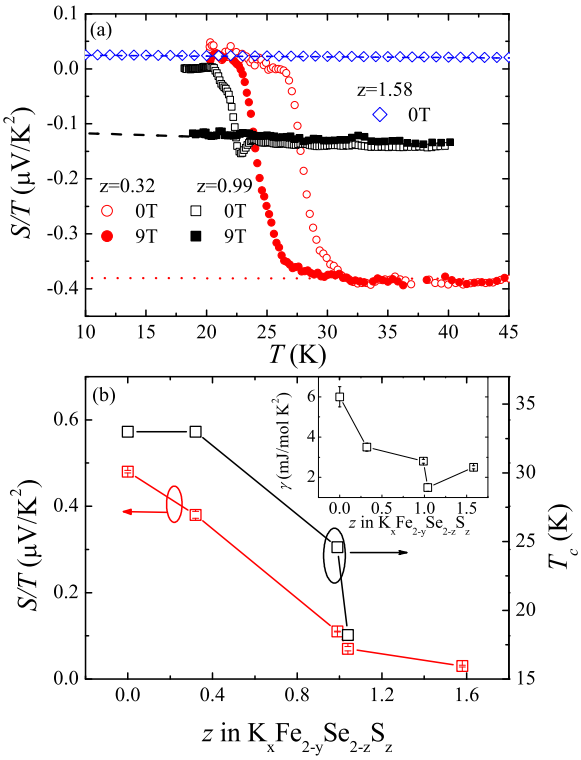

FIG. 3. (Color online) (a) Temperature dependence of the Seebeck coefficient divided by T, $\frac{S}{T}$, for $K_xFe_{2-y}Se_{2-z}S_z$ with $z = 0.32$, 0.99 and 1.58 under 0 T (open symbols) and 9 T (closed symbols), respectively. The dashed lines are the linear fitting results within high temperature range as described in text. (b) The relationship between the zero-temperature extrapolated value of $\frac{S}{T}$ (open circle) and superconducting T_c (open square) to S concentration z in $K_xFe_{2-y}Se_{2-z}S_z$. The inset shows the relationship between the Sommerfeld coefficient and S concentration z in $K_xFe_{2-y}Se_{2-z}S_z$. For superconducting crystals, the Sommerfeld coefficients in normal state induced by magnetic field were used.

and is due to the thermal excitation of carriers over the bandgap. With further increase of temperature, the number of the thermally excited carriers becomes larger and the Seebeck coefficient increases up to ∼180 μV/K^2 at 300 K. For all crystals, there are no evident peaks in the Seebeck curves between 2 K and 300 K, indicating that there is no significant Fermi surface nesting in this temperature range.[25,43,44]

Seebeck coefficient in a material is the sum of three different contributions: the diffusion term S_{diff}, the spin-dependent scattering term and the phonon-drag term S_{drag} due to electron-phonon coupling.[43,45] Thermoelectric power (TEP) in our sample above T_c is independent of magnetic field, which excludes the spin-dependent mechanism. The contribution of phonon-drag term gives $\sim T^3$ dependence for $T << \Theta_D$, $\sim 1/T$ for $T \geq \Theta_D$ (where Θ_D is the

TABLE I. Set of derived parameters for superconducting $K_{0.8}Fe_{2-y}Se_{-z}2S_z$ crystals.

Parameter	$K_{0.64}Fe_{1.44}Se_2$	$K_{0.73}Fe_{1.44}Se_{1.68}S_{0.32}$	$K_{0.70}Fe_{1.55}Se_{1.01}S_{0.99}$	$K_{0.76}Fe_{1.61}Se_{0.96}S_{1.04}$
$\frac{S}{T}$ (μV/K^2)	-0.48(3)	-0.38(8)	-0.11(5)	-0.13(7)
γ (mJ/mol K^2)	6.0(5)[a]	3.5(7)	2.8(7)	1.5(4)
q	0.13	0.09	0.12	0.15
T_c (K)	31.0	31.4	21.4	16.4
T_F (K)	880	1110	3860	3270
$\frac{T_c}{T_F}$	0.04	0.028	0.005	0.005
m^* (m_e)	3.4	2.7	1.1	1.3

[a] The value is obtained from Ref.[50].

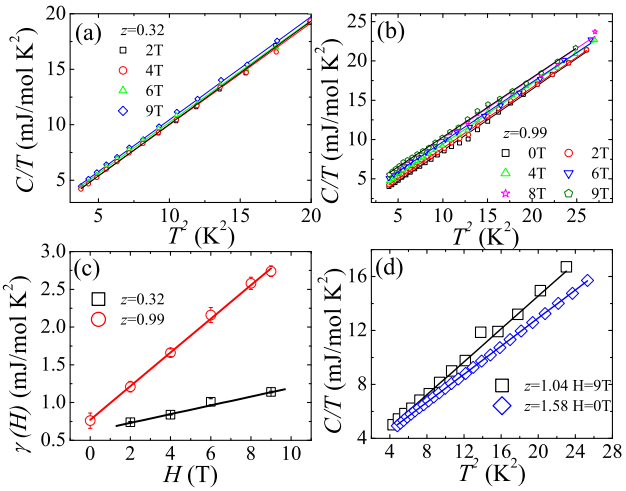

FIG. 4. (Color online) Low temperature specific heat in different magnetic fields up to 9 T for crystals with $z = 0.32$ (a) and $z = 0.99$ (b). The lines are the linear fitting results. (c) Field dependence of the Sommerfeld coefficient $\gamma(H)$ for crystal with $z = 0.32$ (squares) and $z = 0.99$ (circles). (d) Low temperature specific heat data for crystal with $z = 1.04$ in 9 T, and for crystal with $z = 1.58$ in 0 T field, respectively. The lines are linear fitting results.

Debye Temperature), and a peak structure for $\sim \frac{\Theta_D}{5}$.[45] The absence of the peak structure in our TEP results suggests negligible contribution of the phonon drag effect to $S(T)$ since Θ_D for crystals with $z = 0$ and $z = 2.0$ are 260 K and 289 K.[37,44] At low temperature, diffusive Seebeck response of a Fermi liquid dominates and is expected to be linear in T in the zero-temperature limit, with a magnitude proportional to the strength of electron correlations.[42] This is similar to the T-linear electronic specific heat, $C_e/T = \gamma$. In a one-band system both can be described by:

$$S/T = \pm\frac{\pi^2}{2}\frac{k_B}{e}\frac{1}{T_F} = \pm\frac{\pi^2}{3}\frac{k_B^2}{e}\frac{N(\epsilon_F)}{n} \quad (1)$$

$$\gamma = \frac{\pi^2}{2}k_B\frac{n}{T_F} = \frac{\pi^2}{3}k_B^2 N(\epsilon_F) \quad (2)$$

where k_B is Boltzmann's constant, e is the electron charge and n is the carrier density, T_F is the Fermi temperature which is related to the Fermi energy ϵ_F and the density of states $N(\epsilon_F)$ as $N(\epsilon_F) = \frac{3n}{2\epsilon_F} = \frac{3n}{k_B T_F}$.[42] In a multiband system, this gives the upper limit of the Fermi temperature of the dominant band. The Seebeck coefficients of all crystals fit to this formula very well in the low temperature range. Fig. 3(a) shows the relationship between the Seebeck coefficient divided by temperature (S/T) in $K_xFe_{2-y}Se_{2-z}S_z$ with different S content under 0 T and 9 T magnetic field respectively. For superconducting crystals, the Seebeck coefficient in the normal state is independent of magnetic field and exhibits linear relationship with temperature in the low temperature range (Fig. 3(a)). The zero-temperature extrapolated values of S/T for different crystals are shown in Fig. 3(b) and Table I. With sulfur doping, $\frac{S}{T}$ is suppressed from $-0.48\ \mu V/K^2$ to a very small value $\sim 0.03\ \mu$V/K^2 for crystals without superconducting transition. Similar trend was observed in suppression of superconducting T_c (Fig. 3(b)).

Our crystals do not exhibit specific heat anomaly at superconducting transition, similar to previous report and possibly due to the very small superconducting contribution and the nodeless gap.[50] Yet the magnetic field dependent specific heat can yield important information about the Fermi surface. Figs. 4(a) and (b) show the specific heat data plotted as $\frac{C}{T}$ vs T^2 in the low temperature region in different magnetic fields for crystals with $z = 0.32$ and $z = 0.99$ with upper critical field $H_{c2} \sim 45$ T and ~ 13 T (for field applied along the c-axis of the crystals) respecively.[51] The magnetic field gradually enhances the specific heat, indicating the build up of the quasi-particle density of states. From linear fitting to C/T vs T^2 (solid lines in Fig. 4(a) and (b)), we obtained linear dependence of Sommerfeld coefficient on the magnetic field (Fig. 4(c)). This is consistent with the results on $K_xFe_{2-y}Se_2$ and the nodeless gap.[50] The slope of the line in Fig. 4(b)is $\sim 0.06(5)$ mJ/mol K^2 and $\sim 0.22(3)$ mJ/mol K^2 for two crystals with $z = 0.32$ and 0.99 respectively. We estimate the value of normal-state electron specific heat coefficient γ_n to be 3.5 mJ/mol K^2 using upper critical field $H_{c2}(0) \sim 45$T for $z = 0.32$, and $\gamma_n = 2.8(7)$ mJ/mol K^2 for crystal with $z = 0.99$ using $H_{c2}(0) \sim 13$ T respectively.[51] These values are smaller than the value ($\sim 6.0(5)$ mJ/mol K^2) in $K_xFe_{2-y}Se_2$ system as

shown in Table I and the inset of Fig. 3(b).[50] Application of 9 T magnetic field parallel to c-axis completely suppresses the superconductivity in crystal with $z = 1.04$ and we obtain $\gamma_n \sim 1.5$ mJ/mol K^2 directly from the linear fit of the low temperature C/T vs T^2 in 9 T (Fig. 4(d)). For crystal with $z = 1.58$, we extract the Sommerfeld coefficient from zero-field specific heat data (Fig. 4(d)). The results are shown in Table I and the inset of Fig. 3(b). With the increase in sulfur content the electronic Sommerfeld coefficient in the normal state is gradually suppressed.

According to (1) and (2), S/T and the electron Sommerfeld term in specific heat are related to the carrier density and the density of states at the Fermi energy. Since the sulfur has identical electronic configuration to selenium, there should be no change in the carrier concentration with sulfur doping because the elemental analysis is consistent with full occupancy of S(Se) sites.[36] The absolute value of the dimensionless ratio of Seebeck coefficient to specific heat $q = \frac{N_{Av}eS}{T\gamma_n}$ with N_{Av} the Avogadro number, gives the carrier density. From the values of S/T and γ_n obtained previously, we derived q values for four superconducting crystals (Table I). The q values do not exhibit significant change. Therefore the suppression of S/T and γ_n reflects a suppression of density of states at the Fermi level or a change in the Fermi surface.

The ratio of the superconducting transition temperature T_c to Fermi temperature T_F gives information about the correlation strength in superconductors. The ratio $\frac{T_c}{T_F} \sim 0.04$ for $K_{0.64}Fe_{1.44}Se_2$ implies a weakly correlated superconductor.[44] With increase in sulfur content, the value of $\frac{T_c}{T_F}$ decreases as shown in Table I. This implies a suppression of electron correlation strength as the system is tuned towards semiconducting states. The effective mass, m^*, derived from $k_BT_F = \frac{\hbar^2k_F^2}{2m^*}$, is also suppressed with the increase in S content (Table I), consistent with the decrease of correlation strength with S doping. This implies that the neighboring nonmetallic states, such as in $K_{0.88}Fe_{1.63}S_2$, do not originate from strong correlations as in Mott insulator. Moreover, with S increase from 0 to 0.8, $\frac{T_c}{T_F}$ decreases significantly (Table I), but the superconducting T_c survives and is relatively high ($\sim$ 20 K). This indicates that the electron correlations are not strong and do not play a primary role in the superconductivity. Recent first principle calculation point out the gap in the insulating states in proximity to $K_xFe_{2-y}Se_2$ does not depend on the Coulomb repulsive U, implying irrelevance of the Mott insulator scenario. Our results are consistent with this theoretical study.

IV. CONCLUSION

In summary, we studied the evolution of thermal transport and thermodynamic properties of $K_xFe_{2-y}Se_{2-z}S_z$ ($0 \leq z \leq 2$). The zero-temperature extrapolated value of Seebeck coefficient S/T is gradually suppressed, and then undergoes a sharp decrease at $z = 0.99$ to a very small value ($\sim 0.03(2)$ μV/K^2) for crystals with more sulfur content. The electron Sommerfeld term (γ_n) in specific heat also decreases with increase in sulfur content. The suppression of S/T and γ_n reflects a suppression of density of states at the Fermi level or a change of Fermi surface. The ratio $\frac{T_c}{T_F}$ is also suppressed by sulfur doping, indicating the suppression of electron correlations. The superconductivity survives with relatively high T_c even when electron correlations are greatly reduced. This implies that this superconducting system does not lie in the proximity of a Mott insulator and that the electron correlations do not play a primary role in superconductivity.

ACKNOWLEDGMENTS

We than John Warren for help with SEM measurements. Work at Brookhaven is supported by the U.S. DOE under contract No. DE-AC02-98CH10886 and in part by the center for Emergent Supercondcutivity, and Energy Frontier Research Center funded by the U.S. DOE, office for Basic Energy Science.

[1] Y. Kamihara, T. Watanabe, M. Hirano, and H. Hosono, J. Am. Chem. Soc. **130**, 3296 (2008).
[2] I. I. Mazin, Nature **464**, 183 (2010).
[3] D. C. Johnson, Adv. Phys. **59**, 803 (2010).
[4] G. F. Chen, Z. Li, D. Wu, G. Li, W. Z. Hu, J. Dong, P. Zheng, J. L. Luo, and N. L. Wang, Phys. Rev. Lett. **100**, 247002 (2008).
[5] Z. -A. Ren, J. Yang, W. Lu, W. Yi, H. -C. Che, X. -L. Dong, L. -L. Sun, F. Zhou, Z. -X. Zhao, Mater. Res. Innovat. **12**, 1 (2008).
[6] X. H. Chen, T. Wu, G. Wu, R. H. Liu, H. Chen, and D. F. Fang, Nature (London) **453**, 761 (2008).
[7] Z. -A. Ren, W. Lu, W. Yi, H. -C. Che, X. -L. Shen, Z. -C. Li, G. -C. Chen, X. -L. Dong, L. -L. Sun, F. Zhou, Z. -X. Zhao, Chin. Phys. Lett. **25**, 2215 (2008).
[8] C. Wang, L. Li, S. Chi, Z. Zhu, Z. Ren, Y. Li, Y. Wang, X. Lin, Y. Luo, S. Jiang, X. Xu, G. Cao, and Z. Xu, Europhys. Lett. **83**, 67006 (2008).
[9] A. Leithe-Jasper, W. Schnelle, C. Geibel, and H. Rosner, Phys. Rev. Lett. **101**, 207004 (2008).
[10] M. Rotter, M. Tegel, and D. Johrendt, Phys. Rev. Lett. **101**, 107006 (2008).
[11] G. Mu, H. Luo, Z. Wang, L. Shan, C. Ren, and H.-H. Wen, Phys. Rev. B **79**, 174501 (2009).
[12] X. C. Wang, Q. Q. Liu, Y. X. Lv, W. B. Gao, L. X. Yang, R. C. Yu, F. Y. Li, and C. Q. Jin, Solid State Commun. **148**, 538 (2008).
[13] J. H. Tapp, Z. Tang, B. Lv, K. Sasmal, B. Lorenz, Paul C. W. Chu, and A. M. Guloy, Phys. Rev. B **78**, 060505 (2008).
[14] F. C. Hsu, J. Y. Luo, K. W. Yeh, T. K. Chen, T. W. Huang, P. M. Wu, Y. C. Lee, Y. L. Huang, Y. Y. Chu, C. L. Chen, J. Y. Luo, D. C. Yan, and M. K. Wu, Proc. Natl. Acad. Sci. U.S.A. **105**, 14262 (2008).
[15] Y. Mizuguchi, F. Tomooka, S. Tsuda, T. Yamaguchi, and Y. Takano, Appl. Phys. Lett. **94**, 012503 (2009).
[16] I. I. Mazin, D. J. Singh, M. D. Johannes, and M. H. Du, Phys. Rev. Lett. **101**, 057003 (2008).
[17] K. Seo, B. A. Bernevig, and J. Hu, Phys. Rev. Lett. **101**, 206404 (2008).
[18] X. F. Wang, T. Wu, G. Wu, H. Chen, Y. L. Xie, J. J. Ying, Y. J. Yan, R. H. Liu, and X. H. Chen, Phys. Rev. Lett. **102**, 117005 (2009).
[19] V. Cvetkovic and Z. Tesanovic, Euro. Phys. Lett. **85**, 37002 (2009).
[20] M. M. Qazilbash, J. J. Hamlin, R. E. Baumbach, L. Zhang, D. J. Singh, M. B. Maple, and D. N. Basov, Nature Phys. **5**, 647 (2009).
[21] Z. G. Chen, R. H. Yuan, T. Dong and N. L. Wang, Phys. Rev. B **81**, 100502 (2010).
[22] T. Yildirim, Phys. Rev. Lett. 101, 057010 (2008).
[23] D. J. Singh and M. H. Du, Phys. Rev. Lett. 100, 237003 (2008).
[24] Q. Si and E. Abrahams, Phys. Rev. Lett. 101, 076401 (2008).
[25] A. Pourret, L. Malone, A. B. Antunes, C. S. Yadav, P. L. Paulose, B. Fauque, and K. Behnia, Phys. Rev. B **83**, 020504 (2011).
[26] J. Dai, et al., Proc. Nat. Acad. Sci. USA **106**, 4118 (2009).
[27] K. Haule, J. H. Shim, G. Kotliar, Phys. Rev. Lett. **100**, 226402 (2008).
[28] J. G.Guo, S. F. Jin, G. Wang, S. C. Wang, K. X. Zhu, T. T. Zhou, M. He, and X. L. Chen, Phys. Rev. B **82**, 180520 (2010).
[29] J. J. Ying, X. F. Wang, X. G. Luo, A. F. Wang, M. Zhang, Y. J. Yan, Z. J. Xiang, R. H. Liu, P. Cheng, G. J. Ye, X. H. Chen, New J. Phys. **13**, 033008 (2011).
[30] C. H. Li, B. Shen, F. Han, X. Y. Zhu, and H. H. Wen, arXiv:1012.5637 (2010).
[31] A. F. Wang, J. J. Ying, Y. J. Yan, R. H. Liu, X. G. Luo, Z. Y. Li, X. F. Wang, M. Zhang, G. J. Ye, P. Cheng, Z. J. Xiang, and X. H. Chen, Phys. Rev. B **83**, 060512 (2011).
[32] Y. Zhang, L. X. Yang, M. Xu, Z. R. Ye, F. Chen, C. He, J. Jiang, B. P. Xie, J. J. Ying, X. F. Wang, X. H. Chen, J. P. Hu, D. L. Feng, Nature Mater. **10**, 273 (2011).
[33] X.-P. Wang, T. Qian, P. Richard, P. Zhang, J. Dong, H.-D. Wang, C.-H. Dong, M.-H. Fang, H. Ding, Euro. Phys. Lett. **93**, 57001 (2011).
[34] Daixiang Mou, Shanyu Liu, Xiaowen Jia, Junfeng He, Yingying Peng, Guodong Liu, Shaolong He, Xiaoli Dong, Jun Zhang, J. B. He, D. M. Wang, G. F. Chen, J. G. Guo, X. L. Chen, Xiaoyang Wang, Qinjun Peng, Zhimin Wang, Shenjin Zhang, Feng Yang, Zuyan Xu, Chuangtian Chen, X. J. Zhou, Phys. Rev. Lett. **106**, 107001 (2011).
[35] Y. Mizuguchi, Y. Hara, K. Deguchi, S. Tsuda, T. Yamaguchi, K. Takeda, H. Kotegawam, H. Tou, and Y. Takano, Supercond. Sci. Technol. **23**, 054013 (2010).
[36] H. Lei, and C. Petrovic, Phys. Rev. B **83**, 184504 (2011).
[37] H. Lei, M. Abeykoon, E. S. Bozin, and C. Petrovic, Phys. Rev. B **83**, 180503 (2011).
[38] M. H. Fang, et al., Euro. Phys. Lett. **94**, 27009 (2011).
[39] R. Yu, J. X. Zhu, and Q. Si, Phys. Rev. Lett. **106**, 186401 (2011).
[40] X. W. Yan, M. Gao, Z. Y. Lu, and T. Xiang, Phys. Rev. Lett. **106**, 087005 (2011).
[41] W. Yin, C. Lin, and W. Ku, arXiv:1106.0881.
[42] K. Behnia, D. Jaccard, and J. Flouquet, J. Phys.: Condens. Matter **16**, 5187 (2004).
[43] N. Kang, P. Auban-Senzier, C. R. Pasquier, Z. A. Ren, J. Yang, G. C. Chen, and Z. X. Zhao, New J. Phys. **11**, 025006 (2009).
[44] K. Wang, H. Lei and C. Petrovic, Phys. Rev. B **83**, 174503 (2011).

[45] R. D. Barnard, *Thermoelectricity in Metals and Alloys* (Taylor & Francis, London, 1972).
[46] J. G. Checkelsky, L. Li, G. F. Chen, J. L. Luo, N. L. Wang, and N. P. Ong, arXiv:0811.4668.
[47] Y. Machida, K. Tomokuni, T. Isono, K. Izawa, Y. Nakajima, and T. Tamegai, J. Phys. Soc. Jpn. **78**, 073705 (2009).
[48] Y. Zhang, N. P. Ong, P. W. Anderson, D. A. Bonn, R. Liang, and W. N. Hardy, Phys. Rev. Lett. **86**, 890 (2001).
[49] K. Krishana, N. P. Ong, Y. Zhang, Z. A. Xu, R. Gagnon, and L. Taillefer, Phys. Rev. Lett. **82**, 5108 (1999).
[50] Bin Zeng, Bing Shen, Genfu Chen, Jianbao He, Duming Wang, Chunhong Li, Hai-Hu Wen, Phys. Rev. B **83**, 144511 (2011).
[51] Hechang Lei and C. Petrovic, arXiv:1104.2318 (2011).